NUMERICAL ANALYSIS OF INFLUENCE OF DIFFERENT TRACK STRUCTURES ON VIBRATION RESPONSE OF SUBWAY

by

Xin ZHOU [a,b]

[a] School of Civil Engineering, Tianjin University, Tianjin, China
[b] Tianjin Metro Group Co., Ltd., Tianjin, China

Original scientific paper
https://doi.org/10.2298/TSCI190509019Z

Taking Beijing metro line 5 as the research vehicle model, the influence of different track structure on subway vibration is analyzed. According to the coupling dynamic equations of vehicle rail, the coupling dynamic equations of vehicle body models under integrated rail bed, plate rail bed and floating plate rail structure are established, respectively, and the vibration response of vehicle body models under three kinds of rail structure is calculated. The evaluation indexes of dynamic characteristics of rail coupling are analyzed. The analysis results show that with the increase of subway speed, the vertical displacement and acceleration between the vehicle and the middle point of the track gradually increase, and the vibration response of the fourth wheel to the maximum wheel-rail force also gradually increases. With the increase of the buried depth of subway tunnel, the maximum vertical displacement and ground motion acceleration of the three tracks gradually decrease, which indicates that this method can accurately analyze the vibration response of subway under different track structures.

Key words: *different orbits, structural form, subway vibration, response effect, numerical analysis*

Introduction

Metro-based urban rail transit is a fast, environmentally friendly and comfortable mass transit mode of transportation, but the noise caused by rail transit not only affects the surrounding environment, but also directly affects people's lives and health. In order to reduce maintenance time and reduce environmental vibration [1], most of the urban rail transit track structures use ballastless tracks. There are many types of innocent tracks. In the R&D, trial-laying and application process of ballastless track, the state has developed various characteristics of ballastless track structures according to the characteristics of railways, such as monorail beds, plate track beds, floating plate track beds and other track structures. The floating slab ballastless track is effective in absorbing and noise reduction [2, 3], which is suitable for densely populated areas and some special areas. The steel spring floating slab track has been widely used in China. At present, many researchers had analyzed the vibration response of floating slab ballastless tracked in subway tunnels, but rarely compare them with other types of ballastless tracks. At the same time, the lack of consideration of the influence of the structural parameters of the floating slab ballastless track bed on the system vibration requires further research work [4-8].

Author's e-mail: zxclinton@126.com

Based on the previous studies, this paper establishes the vehicle-orbit coupling dynamics model. Under the condition of track harmonics irregularity, the dynamic response of the integrated ballastless track, the slab ballastless track and the floating slab ballastless track in the subway are analyzed and compared, so as to reveal the intrinsic factors affecting the dynamic response and serve as passengers, and provide some reference data for the comfort and stability of the track structure vibration .

Materials and methods

Research object model

Taking the Beijing Metro Line 5 vehicle as the research object, the subway vehicle model consists of one car body, two bogies, four-wheel sets and two layers of suspension systems. The car body is regarded as the rigid body with the mass of M_c and the moment of inertia of J_c around its center of mass. The bogie is considered to be rigid body with the mass of M_1 and the moment of inertia of J_1 [9, 10]. The wheels are considered as rigid bodies with the mass of M_w. The spring stiffness and damping coefficients of the primary suspension are k_{ct} and c_{ct}, respectively, and the spring stiffness and damping coefficients of the secondary suspension are k_{tw} and c_{tw}, respectively. The body freedom is the vertical displacement Z_c and the corner θ_c at the center of mass. The bogie freedom is the vertical displacement Z_{ti} and the angle θ_{ti} at the center of mass (It is the front bogie freedom when $i = 1$, it is the rear bogie freedom when $i = 2$). The wheel pair freedoms are the vertical displacements of the center of mass Z_{w1}, Z_{w2}, Z_{w3} and Z_{w4}, respectively.

Therefore, the vehicle has a total of 10 degrees of freedom , the half of the vehicle is l_c, and the fixed wheelbase of the bogie is l_t.

Different orbital structure models

In the overall track bed dynamics model, the stiffness between the rail and the rigid foundation is k_{rb} and the damping is c_{rb}. According to the structural characteristics of the slab track bed, the track slab is considered to be the free beam supported on the continuously distributed linear spring and linear damping, and the position below the track plate is considered to be the rigid foundation. Each track plate has the length of L_s, The stiffness between the rail and the floating plate is k_p and the damping is c_p. The stiffness between the plate and the rigid foundation is k and the damping is c. According to the structural characteristics of the spring-loaded floating-plate bed, the floating plate is regarded as the finite-length free beam supported on the continuous elastic discrete point, and the floating plate is regarded as the rigid foundation below [11-13]. Each floating plate has the length of L_f. The stiffness between the rigid rail and the floating plate is k_p and the damping is c_p. The stiffness between the floating plate and the rigid foundation is k and the damping is c. The three track bed models all consider the rail as the Euler beam on the elastic point support distributed by the fastener spacing. The interaction between the wheel and rail perpendiculars uses the Hertz non-linear elastic contact model.

Vehicle-track coupling dynamic equation

First, the differential equation of vehicle vibration is established according to the D'Alembert principle. The matrix form is:

$$\left[M_v\right]\left\{\ddot{y}_v\right\}+\left[C_v\right]\left\{\dot{y}_v\right\}+\left[K_v\right]\left\{y_v\right\}=\left[F_v\right] \tag{1}$$

where $[M_v]$, $[C_v]$, and $[K_v]$ are the mass matrix, damping matrix and stiffness matrix of the vehicle respectively, $[F_v]$ is the force vector, and the displacement column vector is:

$$\{y_v\} = [Z_c\ \theta_c\ Z_{t1}\ \theta_{t1}\ Z_{t2}\ \theta_{t2}\ Z_{w1}\ Z_{w2}\ Z_{w3}\ Z_{w4}]^T \tag{2}$$

Then, the vibration equation of the rail is established. Except for the influence of the damping of the rail itself, the dynamic equation can be obtained from the bending dynamics of the Euler beam:

$$E_r I_r \frac{\partial^4 Z_r(x_r,t)}{\partial x_r^4} + m_r \frac{\partial^4 Z_r(x_r,t)}{\partial x_r^2} = \sum_{i=1}^{nr} \delta(x_r - x_{ri}) F_{ri}(t) + \sum_{j=1}^{4} \delta(x_r - x_{wj}) P_j(t) \tag{3}$$

where eq. (4) is:

$$F_{ri}(t) = c_{rb}\left[\dot{Z}_r(x_i,t) - \dot{Z}_{si}(x_i,t)\right] + k_{rb}\left[Z_r(x_i,t) - Z_{si}(x_i,t)\right] \tag{4}$$

where $E_r I_r$ is the bending stiffness of the rail, $P_j(t)$ – the vertical force acting on the rail of the j^{th} wheel pair, nr – the number of fasteners in the track length, x_n – the n^{th} buckle node in the rail. The co-ordinate value on the top, x_{wj} is the co-ordinate value of the j^{th} wheel set. Equation (3) is the fourth-order PDE, which is reduced by the Ritz method. The rail is regarded as the simply supported beam model, and its regular mode function is:

$$T_{rn}(x_r) = \sqrt{\frac{2}{m_r L_r}\sin\left(\frac{n\pi x_1}{L_r}\right)} \tag{5}$$

where L_r is the rail length. Then the solution of eq. (3) can be expressed:

$$Z_r(x_r,t) = \sum_{n=1}^{N_r} T_{rn}(x_r) q_{rn}(t) \tag{6}$$

where N_r is the modal order intercepted, $q_{rn}(t)$ – the regular co-ordinate. Substituting the eq. (6) into the eq. (3), multiplying the various modes by the two sides, and then integrating.

According to the Ritz method, the vertical displacement of the track plate can be expressed:

$$Z(x,t) = \sum_{n=1}^{NM} X_n(n) T_n(t) \tag{7}$$

where $T_n(t)$ is the generalized co-ordinate, X_n – the function system of the free beam, $X_1 = 1$, $X_2 = 3^{1/2}(1 - 2x/L_s)$, $X_m = (\text{ch}\beta_m x + \cos\beta_m x) - C_m(\text{sh}\beta_m x + \sin\beta_m x), (m > 2)$, m – the modal order, C_m – the beam function coefficient, β_m – the beam frequency coefficient. Here $C_3 = 0.982502$, $\beta_3 L_s = 0.72004$, $C_4 = 1.0000777$, $\beta_4 L_s = 7.853$, $C_5 = 0.999966$, and $\beta_5 L_s = 10.9956$. When $m \geq 6$, $C_m = 1$ and $\beta_m L_s = (2m - 3)/\pi$.

Substituting eq. (11) into eq. (8) and multiplying $X_k(k = 1 \sim NM)$ on both sides of the equation. Then, the integral along the length of the plate, the vibrational equation satisfied by the generalized co-ordinates of the track plate obtained by the modal orthogonality and the δ function property is:

$$\rho L_s \ddot{T}_n(t) + EI\beta_n^4 L_s T_n(t) = \sum_{i=1}^{nr} F_{rsi}(t) X_n(x_{ri}) - \sum_{j=1}^{n} F_{ssj}(t) X_n(x_{sj}) \tag{8}$$

Similarly, the vibration equation of the floating plate can be obtained:

$$\rho_f L_f \ddot{T}_n(t) + E_f I_f \beta_n^4 L_f(t) = \sum_{i=1}^{nr} F_{rfi}(t) X_n(x_{ri}) - \sum_{j-1}^{ns} F_{fsj}(t) X_n(x_{sj}) \tag{9}$$

where E_f and I_f are the bending stiffness of the floating plate, ρ_f – the mass per unit length of the floating plate, NMS – the cut-off mode order, L_f – the length of the floating plate, ns – the number of steel springs.

The rail fulcrum reaction force $F_{rfi}(t)$ and the steel spring fulcrum force $F_{fsi}(t)$ are as eqs. (10) and (11):

$$F_{rfi}(t) = c_p\left[\dot{Z}_r(x_i,t) - \dot{Z}_{si}(x_i,t)\right] + k_p\left[Z_r(x_i,t) - Z_{si}(x_i,t)\right] \tag{10}$$

$$F_{fsi}(t) = c_s \dot{Z}_s(x_i,t) + k_s Z_s(x_i,t) \tag{11}$$

where k_s and c_s is the stiffness and damping of the steel spring, k_p and c_p – the stiffness and damping of the rail fastener, and $Z_s(x,t)$ and $\dot{Z}_s(x,t)$ – the vertical displacement and velocity of the floating plate.

The wheel-rail contact relationship can be determined by the Hertz non-linear elastic contact theory. When the wheel-rail interface has a displacement irregularity $Z_0(t)$ inputs, the wheel-rail force expression is:

$$p_i(t) = \left\{\frac{1}{G}\left[Z_{wi}(t) - Z_r(x_{wi},t) - Z_0(t)\right]\right\}^{3/2} \tag{12}$$

where G is the wheel-rail contact constant $(mN^{-2/3})$. For the wheel-type tread wheel, $G = 3.68R^{-0.115} \cdot 10^{-8} mN^{-2/3}$, Z_0(t) is the local surface irregularity of the rail. In many cases, the track set is not smooth and can be approximated by a single or multiple simple harmonic.

Evaluation index of vehicle-track coupling dynamics

The smooth running of the vehicle is usually used to indicate the vibration performance of the vehicle. It is an important technical indicator to measure the running performance of the vehicle. It is generally expressed by the vibration acceleration and comfort of the vehicle body.

(1) Vehicle body vibration acceleration index

When the running speed of the train is assessed by the average maximum vibration acceleration of the vehicle body, according to national regulations, when the subway running speed is lower than 140 km/h, the average maximum vibration acceleration of the vehicle body should meet:

$$\overline{A}_{\max} \le 0.00027v + C \tag{13}$$

where $\overline{A}_{\max}$ represents the average maximum vibration acceleration of the vehicle body, v [kmh^{-1}] – the running speed of the subway, C – the constant, and the calculation constant of the average maximum vibration acceleration of the subway is shown in tab. 1.

(2) Comfort index

Passenger comfort is a comprehensive physiological indicator that reflects passengers and is the statistical standard. There are many factors that affect passenger comfort, such as ventilation inside the car, temperature noise, vibration, *etc*. Among them, vibration is one of the main factors that always exist and always play the role in the whole operation of the vehicle. Japan uses the equal comfort method (Janeway comfort coefficient J =1-1.5) as the evaluation standard. Most countries tend to use the stability index method (Sperling comfort index W) as the evaluation standard. China's vehicle research and manufacturing departments use the former. According to the vertical and lateral vibration, the boundary values of various frequency ranges are connected into the curve, that is, the comfort curve, and they are used as the reference to calculate the level of comfort level J:

Table 1. Calculation constants of average maximum vibration acceleration of metro

Running smoothness level	C	
	Vertical vibration	Transverse vibration
Excellent	0.025	0.01
Good	0.03	0.018
Qualified	0.035	0.025

$$J(A, f) = \frac{A}{F(f)} \tag{14}$$

where $J(A, f)$ and A are multiples of the acceleration g, $F(f)$ – the function expression of the two limit curves.

This paper is based on the comfort method, and the calculated calculation index of the stationarity index is described in tab. 2.

Table 2. Frequency correction coefficients for calculating stationarity indicators

Comfort level	Excellent	Good	Commonly	Poor	Very poor
Level of stationarity J	< 1	1-1.5	1.5-2	2-3	> 3

Results

Influence of distance from subway centerline on vibration response of different track structures

The grounds at 10 m, 15 m, 20 m, and 25 m from the centerline of the subway tunnel were selected and simulated. The results are shown in figs. 1 and 2. Figure 1 shows the ground vibration displacement at different distances from the centerline of the subway. Figure 2 shows the ground vibration acceleration at different distances from the centerline of the subway.

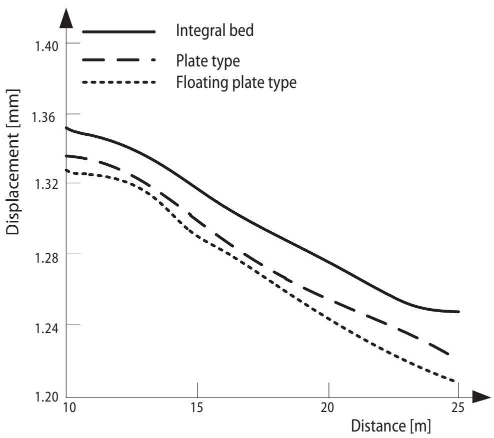

Figure 1. Ground vibration displacement at different distances from the subway center line

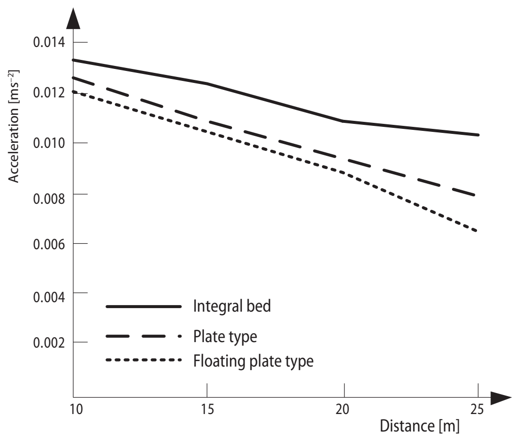

Figure 2. Ground vibration acceleration at different distances from the subway center line

The method analysis shows that the maximum vertical displacement of the ground vibration of the three track structures decreases with the increase of the distance from the centerline of the subway. In the range of 10-20 m from the centerline of the tunnel, the vertical displacement of the ground vibration is greatly reduced. On the other hand, more than 20 m away from the center line of the subway, the vertical displacement of the ground vibration decreases with the increase of the distance. It can be seen from fig. 2 that the method analysis shows that with the increase of the distance from the centerline of the subway, the maximum vertical acceleration of the ground vibration of the three tracks gradually decreases, reaching a minimum at 25 m from the centerline of the tunnel.

Influence of buried depth on the vibration response of the ground

In order to analyze the influence of the tunnel depth on the vibration response of the ground, the grounds with the depth of 14 m, 16 m, 18 m, and 20 m and the distance of 15 m from the centerline of the subway are simulated. And the response analysis results are described by figs. 3 and 4, respectively.

It can be seen from fig. 3 that the method analysis shows that with the increase of the buried depth of the subway tunnel, the maximum vertical displacement of the ground vibration of the three tracks gradually decreases. It can be concluded from fig. 4 that the method analysis shows that with the increase of the buried depth of the subway tunnel, the maximum vertical acceleration of the ground vibration of the three tracks gradually decreases. The attenuation of the acceleration tends to be gentle with the increase of the buried depth. Therefore, increasing the buried depth of the subway tunnel can improve the ground vibration acceleration within a certain range. From the economic point of view, the economic benefits of excessively increasing the buried depth are poor.

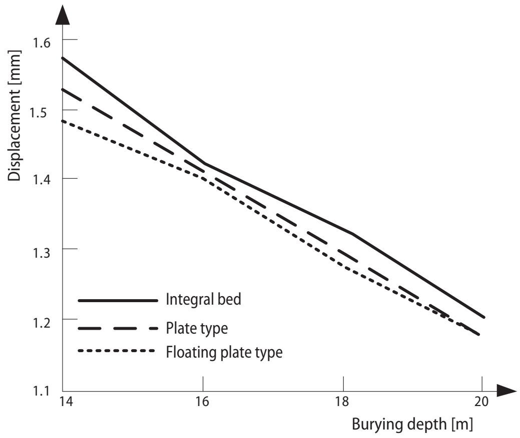

Figure 3. Influence of different burial depths on ground vibration displacement

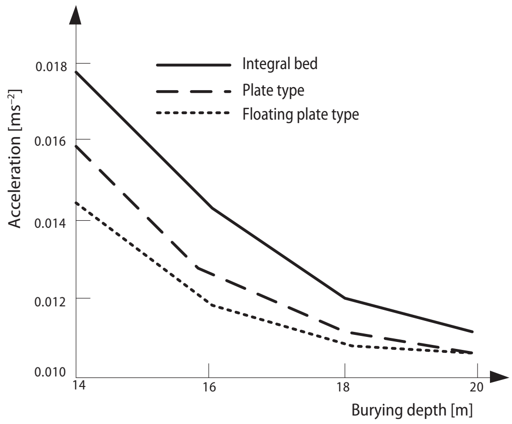

Figure 4. Ground vibration acceleration at different burial depths

Conclusion

In this study, it is verified that the vibration response of the three kinds of track structures under the subway operating conditions increases with the increase of vehicle speed under the proposed method. When the speed is constant, the vertical displacement of the vehicle body, the vertical acceleration of the vehicle body and the maximum elastic force of the foundation are the least. Therefore, under the floating plate rail bed structure, the subway has higher comfort. According to the response results of subway tunnel to ground vibration, deepening subway depth can reduce ground vibration displacement and acceleration. However, in order to improve the economic efficiency of subway, it needs to be controlled within a certain range.

References

[1] Ogierman, W., *et al*., A Study on Fiber Orientation Influence on the Mechanical Response of a Short Fiber Composite Structure, *Acta Mechanica, 227* (2015), 1, pp. 1-11

[2] Freour, V., *et al*., Numerical Investigation on the Influence of Wall Vibrations on the Behavior of the Lip Excitation in Brass Instruments, *Journal of the Acoustical Society of America, 140* (2016), 4, pp. 3037-3037

[3] Che, Y., *et al*., The Influence of Different Constraints and Pretightening Force on Vibration and Stiffness in Railgun, *IEEE Transactions on Plasma Science, 45* (2017), 7, pp. 1-7

[4] Cao, L., *et al*., Influence of Solid Particle Erosion (SPE) on Safety and Economy of Steam Turbines, *Applied Thermal Engineering*, *150* (2019), Mar., pp. 552-563

[5] Wang, L., *et al*., Influence on Vibration and Noise of Squirrel-cage Induction Machine with Double Skewed Rotor for Different Slot Combinations, *IEEE Transactions on Magnetics, 52* (2016), 7, pp. 1-4

[6] Duan, M., *et al*., A Application of LSSVM Algorithm for Estimating Higher Heating Value of Biomass Based on Ultimate Analysis, *Energy Sources Part A-Recovery Utilization and Environmental Effects, 40* (2018), 6, pp. 709-715

[7] Ibrahim, M. D., *et al*., Characteristics of Modified Spiral Thrust Bearing through Geometries and Dimension Modifications, *Tribology Online*, *13* (2018), 6SI, pp. 334-339

[8] Vilkov, L. V., *et al*., The Influence of Torsional Vibrations on the Molecular Configuration Determined by Gas Electron Diffraction, *Journal of Molecular Structure, 43* (2015), 1, pp. 109-115

[9] Selmane, A., *et al*., Influence of Geometric Non-linearities on the Free Vibrations of Orthotropic Open Cylindrical Shells, *International Journal for Numerical Methods in Engineering, 40* (2015), 6, pp. 1115-1137

[10] Ning, Z., *et al*., Remarkable Influence of Slack on the Vibration of a Single-walled Carbon Nanotube Resonator, *Nanoscale, 8* (2016), 16, pp. 8658-8665

[11] Ouadhani, S., *et al*., Influence of Vertical Vibrations on the Stability of a Binary Mixture in a Horizontal Porous Layer Subjected to a Vertical Heat Flux, *Transport in Porous Media, 124* (2018), 1, pp. 203-220

[12] Khalique, C. M. *et al*., Travelling Waves and Conservation Laws of a (2+1)-dimensional Coupling System with Korteweg-de Vries Equation, *Applied Mathematics & Nonlinear Sciences*, *3* (2018), 1, pp. 241-254

[13] Pandey, P. K., A New Computational Algorithm for the Solution of Second Order Initial Value Problems in Ordinary Differential Equations, *Applied Mathematics & Nonlinear Sciences*, *3* (2018), 1, pp. 167-174

Paper submitted: May 9, 2019
Paper revised: September 2, 2019
Paper accepted: September 15, 2019